ECRONICON OPEN ACCESS

EC PROTEOMICS AND BIOINFORMATICS
Research Article

Functional Proton Magnetic Resonance Spectroscopy of Cerebral Water and Metabolites using Eight Radiofrequency Excitations at 3.0 Tesla

Abdul Nashirudeen Mumuni* and John Mclean

MRI/SPECT Unit, Institute of Neurological Sciences, Southern General Hospital, Glasgow, United Kingdom

***Corresponding Author**: Abdul Nashirudeen Mumuni, Department of Biomedical Laboratory Sciences, School of Allied Health Sciences, University for Development Studies, Tamale, Ghana.

Received: August 13, 2017; **Published:** August 29, 2017

Abstract

Background: MRS acquisition focusing on the blood oxygenation level dependent (BOLD) contrast mechanism was implemented in this study to investigate the impact of spectral averaging (determined by the number of RF excitations, NEX) on the dynamics of cerebral metabolism during neuroactivation.

Materials and Methods: Using NEX = 8, the BOLD effects on cerebral water and six metabolites were studied at 3.0 T. Spectra were recorded from the visual cortex of four healthy volunteers during single and interleaved visual stimulations.

Results: Generally, single stimulation was found to induce greater BOLD effects on the water and metabolite resonances than interleaved stimulation ($p = 0.02$). The water resonance showed significant ($p < 0.01$) increase in peak height (18.4%) and decrease in linewidth (-3.5%) in the single, but not in the interleaved stimulation. The water peak area however did not change significantly in both stimulation paradigms. Only Cr showed significant linewidth decrease (-3.1%) in the interleaved stimulation paradigm ($p = 0.04$). In the single stimulation paradigm, both NAA (11.2%; $p = 0.01$) and Cr (7.2%; $p = 0.02$) showed significant increases in their peak areas, while Cho was the only metabolite that showed significant increase in its peak height (2.2%; $p = 0.01$). Glu, Gln, and mI did not show significant BOLD responses in both paradigms ($p > 0.05$).

Conclusion: The results of this study were consistent with previous studies at higher fields, indicating that NEX = 8 could improve accuracy of functional MRS studies at lower fields and at the same time offer quicker spectral averaging.

Keywords: *BOLD; Magnetic Resonance Spectroscopy; Brain; NEX; Visual Stimulation; Metabolites*

Abbreviations

A/P: Anterior-Posterior Direction; B_0: Field Strength; BOLD: Blood Oxygen Level Dependent; CHESS: CHEmical Shift Selective Preparation; Cho: Choline; Cr: Creatine; FID: Free Induction Decay; fMRI: Functional Magnetic Resonance Imaging; fMRS: Functional Magnetic Resonance Spectroscopy; FOV: Field-of-View; GE: General Electric; Gln: Glutamine; Glu: Glutamate; mI: Myo-Inositol; MR: Magnetic Resonance; MRI: Magnetic Resonance Imaging; MRS: Magnetic Resonance Spectroscopy; NAA: N-Acetyl Aspartate; NEX: Number of Radiofrequency Excitations; NSA: Number of Signal Averages; PRESS: Point-RESolved Spectroscopy; RF: Radiofrequency; R/L: Right-Left Direction; SAGE: Spectroscopy Analysis by GE; SE: Standard Error; S/I: Superior-Inferior Direction; SNR = Signal-to-Noise Ratio; T_2*: Relaxation Time Constant due to Susceptibility Effects; TE: Echo Time; TR: Repetition Time

Introduction

Functional magnetic resonance imaging (fMRI) based on the blood oxygenation level dependent (BOLD) contrast mechanism has become a common neuroimaging method in research [1-3]. However, there is increasing interest in recent times in probing the dynamics of

brain tissue metabolism during neuroactivation using magnetic resonance spectroscopy (MRS). Even though the MRS technique normally provides information about brain tissue metabolism, it can be used to study brain function in both healthy and pathological conditions, also based on the BOLD contrast [4-8]; this is known as functional MRS (fMRS). The fMRS technique thus offers a new opportunity for neurochemistry and neuroscience research [9].

The BOLD effect can be observed when an external stimulus increases neural activity above baseline physiological state. The new physiological state is associated with changes in cerebral blood flow, cerebral blood volume and the cerebral metabolic rate of oxygen consumption [4]. This increases the flow of oxygenated blood to the region of activity, causing susceptibility gradients to spread around and away from the activation site [5]. This susceptibility gradient, associated with changes in T_2^*, can be detected in vessels (intravascular compartment) and tissue near the vessels (extravascular compartment).

At magnetic fields less than 1.5 T, and in the presence of small bipolar diffusion gradient, the BOLD effect mostly originates from the intravascular compartments in noncapillary vessels and is cancelled out completely through spin dephasing. However, at magnetic fields above 3.0 T, and in the presence of higher bipolar diffusion gradient [10,11], the BOLD effect mostly originates from the extravascular compartment and does not disappear. The extravascular BOLD effect is thus most desirable for mapping locations of functional activation [6]. The BOLD effect has also been observed to increase with field strength [12] due to increased sensitivity of signal detection at high magnetic fields [13].

In fMRI, the BOLD effect often appears as increased intensity in voxels that coincide with the site of the neural activity. In fMRS, the effect manifests as increased spectral peak area and height, corresponding with decreased spectral linewidth [6-8]. The detailed theory of fMRS underpinning the changes in these spectral parameters is described elsewhere [6].

It has been suggested [9] that studies using similar fMRS paradigms, stimulus type, spectral analysis and quantification schemes, assuming high SNR of spectra, should observe comparable BOLD changes. However, what has not been considered in the literature is whether variations in the number of radiofrequency excitations (NEX) used in a particular fMRS study could impact on the BOLD signal. The NEX value is particularly important because it is the time interval between successive spectral lines in the frequency domain; it thus determines the number of spectral lines that will be averaged and stored (in the data frame) within the total duration of the fMRS data acquisition according to:

$$N_{Total} = 16/NEX + NSA/NEX \quad \text{[Equation 1]}$$

where N_{Total} is the number of spectral lines stored in the data frame, NSA is the number of signal averages, (16/NEX) is the number of unsuppressed-water spectral lines, and (NSA/NEX) is the number of suppressed-water spectral lines. The standard PRESS sequence on the GE MR scanner acquires 16 averages of unsuppressed-water lines prior to acquisition of the metabolite spectra.

NEX can be varied between only 2 and 8 on the MR scanner used for this study. However, NEX = 8 is commonly used in standard MRS acquisitions because it allows for the maximum number of spectral lines to be quickly averaged before the FIDs are stored, thus reducing the potential degradation of spectra due to motion effects [14]. Despite these advantages of NEX = 8 for MRS, it has not been reported if using NEX = 8 in fMRS could have any impact on the amount of BOLD signal observed.

In this fMRS study, the BOLD effects on brain tissue water and metabolites were recorded during sustained visual stimulation of the primary visual cortex (V1) of the normal human brain. The aim was to investigate BOLD signal changes (from baseline) in the respective MR spectra, using the conventional number of RF excitations (i.e. NEX = 8), which determines how the MR spectra are averaged. The observed percentage BOLD changes were then compared to those reported in the literature as a means of validation.

Materials and Methods

Subjects

Following ethical approval of the study by the West of Scotland Research Ethics Committee 4 (WoSREC4), 4 healthy volunteers (3 males/1

female, aged 29 - 36 years, mean ± SD = 32.3 ± 3.0 years) participated in the study. Each volunteer gave prior informed written consent. No volunteer had any neurological or psychiatric disorder. Volunteers were screened for contraindicated MRI implants.

Visual Stimulus

A rate of pattern presentation of about 7.8 reversals per second (or 7.8 Hz) has been shown by a previous positron emission tomography (PET) study [15] to induce the maximum blood flow response in the visual cortex. A number of fMRS studies [6,16-18] have thus used stimulus reversal frequency of about 8 Hz. Therefore, an in-house 8 Hz black/white pattern-reversal checkerboard was used for visual stimulation in this study. During the rest period, a black background was displayed. In the rest and stimulation displays, a small fixation cross was centrally placed. Patients were asked to focus on the fixation cross during scanning to ensure that they were attentive during scanning. This also served to ensure that patients focused on a consistent position on the screen throughout scanning. There was no background illumination within the scanner room throughout the experiments.

The rest and stimulation displays were each presented using Windows Media Player (Microsoft Corporation, USA, 2006). Each display was projected from a screen panel that has image transmission cables passing through an observation window into the magnet room, where the projected image is displayed on bifocal lenses. The lens ensemble (Nordic Neurolabs, NNL; http://www.nordicneurolab.com) was attached to the head coil and positioned vertically above (at 90^{o}), but close to, the eyes of the volunteer. For each volunteer, the foci of the lenses were adjusted until they could see a single projected and sharp image through both lenses, simultaneously.

Functional MRI

Functional MR imaging and spectroscopy acquisitions were performed on a 3.0 T GE Signa HD MRI/MRS scanner (software version 12.5; Milwaukee, WI, USA) equipped with an eight-channel receive-only head coil. A preceding fMRI scan was performed on each volunteer to determine the location and size of the activated V1 area. Using this information, a localised voxel for acquiring the fMRS data was then prescribed (Figures 1a-b [19]).

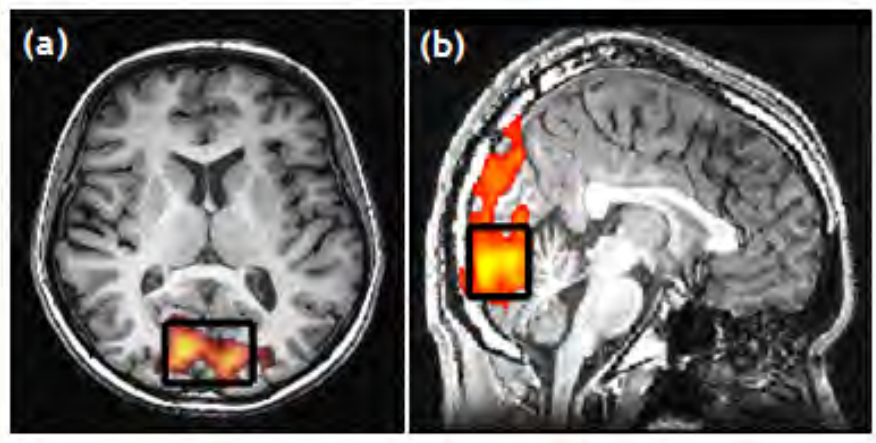

Figure 1: *Axial (a) and sagittal (b) views of the localised fMRS voxel (volume = 20 SI x 20 AP x 30 RL mm^3) within the activation map generated in the V1 brain region during the fMRI examination.*

Functional MRS

The standard spin-echo PRESS sequence on the GE MR scanner [19] acquires 8 dummy scans, followed by 16 averages of unsuppressed-water scans before the actual data acquisition. During the dummy scan, the scanner starts running but no data is stored; only scanner tuning and voxel shimming are performed. Taking the first two non-data (a total of 24 averages) acquisition periods into consideration, the total running time (T_{acq}) of the sequence is given by:

T_{acq} = TR x (24 + NSA) [Equation 2]

Using a repetition time, TR of 3 s throughout the experiments, the duration of visual stimulation (T_{sti}) was therefore synchronised with the actual data acquisition period (i.e. the TR x NSA part of Equation 2) as follows:

$T_{sti} = T_{acq} - 72$ s [Equation 3]

The implication of Equation 3 is that visual stimulation should commence 72 s after the PRESS sequence starts running, in theory. However, in implementation, a black background with a fixation cross was shown 63 s (i.e. 9 s earlier) from the start of the sequence. This 9 s deadtime served two purposes [20]. Firstly, it reduced the possibility of a movement artifact which will arise due to the subject flinching when the lighting level changed suddenly between stimulation and resting conditions. Secondly, within the deadtime period, the changing blood flow stabilises as it alternates between the stimulus and rest periods. This transient response time is about 6.5 - 8 s risetime, with falltime duration within 7-9 s [20,21].

Two visual activation paradigms were designed for the fMRS experiments: one with a rest period followed by a stimulation period of equal duration in separate scans (Table 1); and another with interleaved three rest and three stimulation periods of equal durations within the same scan (Table 2). In this report, the former will be called a "single" stimulation paradigm, and the latter a "block" stimulation paradigm.

Acquisition parameters	**OFF**	**ON**	**Total**
NSA	64	64	128
T_{sti} (s)	192	192	384
T_{acq} (s)	264	264	528

Table 1: *Data acquisition parameters used in the single stimulation paradigm.*

ON: Rest; OFF: Stimulation

Acquisition parameters	**OFF**	**ON**	**OFF**	**ON**	**OFF**	**ON**	**Total**
NSA	32	32	32	32	32	32	192
T_{sti} (s)	96	96	96	96	96	96	576
T_{acq} (s)	108	108	108	108	108	108	648

Table 2: *Data acquisition parameters used in the block stimulation paradigm.*

ON = Rest; OFF = Stimulation

A single-voxel (20 SI x 20 AP x 30 RL mm^3) PRESS localisation sequence was used in the fMRS experiments (Figure 1). Outer-volume and CHESS water suppression techniques were incorporated in the PRESS sequence. The PRESS acquisition parameters were: TE = 23 ms,

TR = 3000 ms, and spectral width = 5000 Hz. In all experiments, NEX = 8 was maintained. The single paradigm was of the form OFF-ON (Table 1), whereas the block paradigm was OFF-ON-OFF-ON-OFF-ON (Table 2); where OFF and ON mean the rest and stimulus periods, respectively.

The metabolite spectra were recorded first with the CHESS water suppression module turned on. The acquisition protocol was then repeated but with CHESS water suppression turned off to acquire the water spectra. Both water and metabolite data were collected using the single and block paradigms in turn. Thus, each volunteer in the study underwent four fMRS scans continuously within an experimental session. In order to ensure consistent voxel placement in all volunteers, the activated V1 region during fMRI was located in the same slice number during fMRS of all volunteers. This did not completely eliminate the potential for voxel placement variations, but served to reduce voxel placement mismatch between scans to about 10% or less.

Spectral Analysis

Since the rest and stimulation periods were synchronised with the duration of actual data acquisition by the scanner, the fMRS information, N_{BOLD} was stored in the (NSA/NEX) part of equation 1:

$N_{BOLD} = NSA/NEX$ [Equation 4]

Using NEX = 8 in all experiments, NSA = 64 in the single paradigm resulted in N_{BOLD} = 8 spectral lines in each of the OFF and ON data. NSA = 192 in the block paradigm yielded N_{BOLD} = 24 spectral lines (4 lines in each of the 6 blocks). These stored lines were processed to estimate the BOLD changes in the acquired spectra.

All spectra were processed and quantified using the Spectroscopy Analysis by General Electric, SAGE software package (version 7; GE Healthcare, Little Chalfont, Buckinghamshire, UK), a dedicated semi-automated fitting program. The time domain signals from the eight channels of the head coil were eddy-current corrected and combined [22]. The resulting time-domain FIDs were Fourier transformed to yield the MR spectra, which were then phase and baseline corrected in the frequency domain.

Spectral processing involved manually selecting (in the frequency domain) those resonances to be quantified. A table of initial estimates of the peak amplitude, linewidth, frequency, and the noise standard deviation of the spectrum was then automatically generated. Using these four variables, the initially generated spectra were then fitted to Lorentzian line shapes using the Levenberg-Marquardt method of nonlinear least squares minimization [23]. This yielded the final peak parameters required for the BOLD investigations in this study: height, linewidth and area of the peak.

The Levenberg-Marquardt method was implemented in two ways. Firstly, each line in the spectral domain was quantified by invoking a "local" quantification algorithm that utilises the Levenberg-Marquardt method. The "local" Levenberg-Marquardt method ensures that the same processing and quantification steps (described above) are applied to each spectral line, separately. Secondly, all the spectral lines were averaged by invoking a "global" Levenberg-Marquardt method. Both quantification schemes yielded the peak height (H), linewidth at half peak height ($\Delta\upsilon_{1/2}$), and spectral peak area (A_s). The "locally" quantified spectral parameters (i.e. H, $\Delta\upsilon_{1/2}$ and A_s) were used to plot the respective time courses of their changes over the cycle duration (Figures 2, 3 and 4). The "globally" quantified spectral parameters on the other hand were used to quantify their respective BOLD responses (i.e. percentage changes in H, $\Delta\upsilon_{1/2}$ and A_s), shown in Tables 3-5.

Estimation of the BOLD Effect

The BOLD effect is associated with increase in peak height (H) following stimulation, with a corresponding decrease in linewidth ($\Delta\upsilon_{1/2}$) and increase in area (A_s). Thus, the BOLD effects on each one of these spectral parameters were calculated as a percentage change:

$\%\Delta X = [(X_{stimulation} - X_{rest})/X_{rest}] \times 100\%$ [Equation 5]

where $X_{stimulation}$ and X_{rest} are the spectral peak parameters associated with the stimulus and rest periods respectively, estimated using the "global" Levenberg-Marquardt method.

Statistical Analysis

The paired t-test was used to compare percentage changes in spectral height, linewidth and area between the rest and stimulation periods in each paradigm. Inter-paradigm comparisons were also done using the paired t-test. Only p-values less than 0.05 were considered significant differences in the comparisons. Statistical tests were performed using the Minitab software package (version 16, Minitab Inc., State College, Pennsylvania, USA).

Results

BOLD Effect on the Water Resonance

The time courses of cerebral water fMRS for the single and block paradigms are shown in Figures 2 and 3, respectively. In figure 2, eight data points are plotted for each one of the rest and stimulation periods; each data point represents the average of the heights of eight spectral peaks, automatically done by the MR scanner during spectral acquisition using NEX = 8. Using TR = 3 s, each data point was then acquired within a time scale of 24 s: thus, during the rest period, the first eight-averaged spectra (from each volunteer) were acquired in 24 s, the next average was acquired 24 s after the first, that is, in 48 s. Thus, the sequence of acquisition times were 24, 48, 72,... 192 s during the rest period, and 216, 240, 264,... 384 s during the stimulation period.

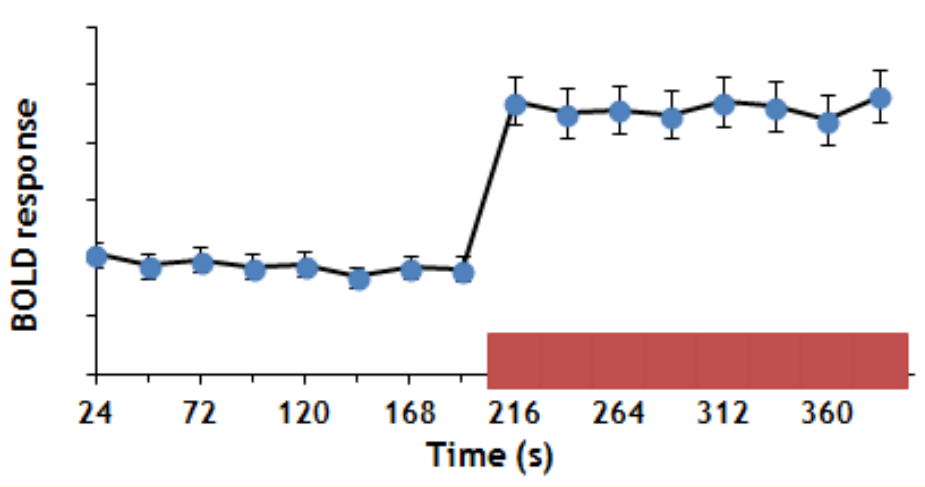

Figure 2: *Time course of the BOLD response (%ΔH) of cerebral water during the single stimulation paradigm.*

In figure 3, each data point again represents an average height of eight spectral peaks, each average acquired within a time scale of 24 s. Thus, each block, comprising four data points, has duration of 96 s, and so the total duration for the six blocks is 576 s.

The plotted data points in figures 2 and 3 are averages from the four volunteers; the error bars represent standard deviations. The rectangular blocks on the time axes indicate the task period of visual stimulation corresponding to the BOLD response.

The BOLD effects on the water resonance are summarised as percentage changes in the height (H), linewidth ($\upsilon_{1/2}$) and area (A_S) of the water peak in table 3. The percentage changes in H, $\upsilon_{1/2}$ and A_S of the water peak are shown for each of the four volunteers. The mean percentage BOLD effects (± standard error, SE) in all four volunteers for both single and block paradigms are also shown.

Generally, significant BOLD effects were observed in the water peak height and linewidth ($p < 0.01$ in both cases) in the single, but not in the block stimulation paradigm. These significant effects however were not associated with significant increase in the water peak

area; the percentage increase in the area of the water peak was not also significant with the block paradigm. Consequently, the mean BOLD response (%ΔH) with the single paradigm was significantly greater than that with the block paradigm (p = 0.02). However, the corresponding mean decreases in linewidth, $\%\Delta\upsilon_{1/2}$ (p = 0.12), and increase in peak area, $\%\Delta A_S$ (p = 0.16) were not significantly different between the two paradigms.

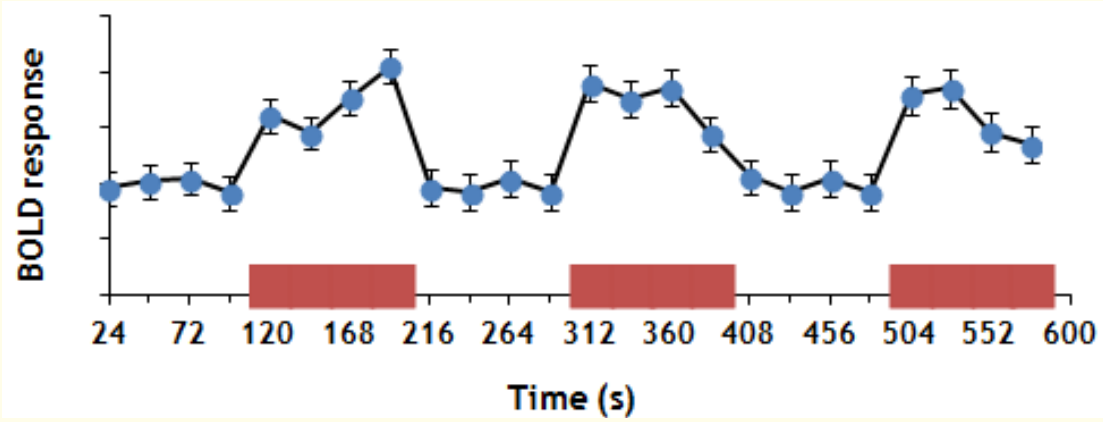

Figure 3: *Time course of the BOLD response (%ΔH) of cerebral water during the block paradigm.*

Volunteer	ΔH (%)		$\Delta\upsilon_{1/2}$ (%)		ΔA_S (%)	
	Single	Block	Single	Block	Single	Block
A	20.52	0.27	-7.20	-0.01	0.10	0.01
B	14.77	0.05	-4.87	-0.04	0.31	0.08
C	9.93	0.13	-1.28	-0.02	0.07	0.05
D	28.25	0.10	-0.45	-0.02	0.89	0.31
Mean ± SE	18.37 ± 3.94	0.14 ± 0.05	-3.45 ± 1.58	-0.02 ± 0.01	0.34 ± 0.19	0.11 ± 0.07

Table 3: *BOLD effects on the cerebral water resonance during visual stimulation.*

BOLD Effect on the Metabolite Resonances

Figure 4 shows the BOLD response patterns of six metabolite resonances during the single stimulation paradigm.

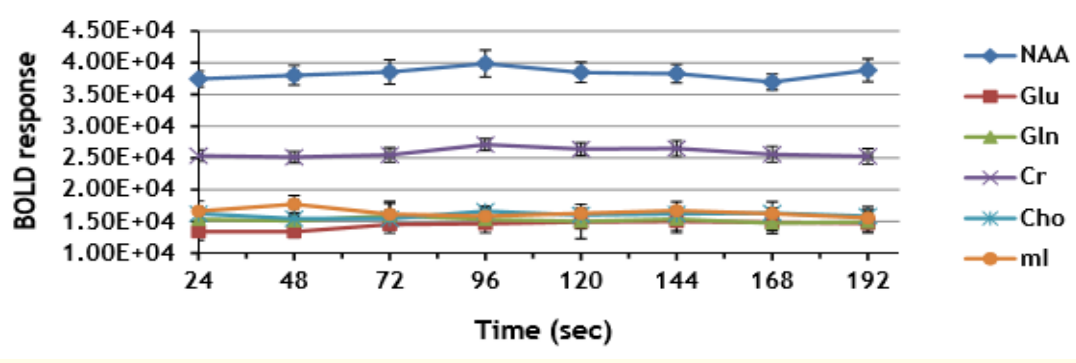

Figure 4: *Temporal evolution of BOLD responses in the metabolite resonances during visual stimulation in the single paradigm.*

Table 4 shows the mean BOLD effects on the metabolite resonances of higher relative abundance (i.e., NAA, Cr, and Cho) from the four volunteers. The significance of each average change is denoted by a p-value in parenthesis.

Only Cr showed a significant linewidth decrease in the block stimulation paradigm (p = 0.04). In the single stimulation paradigm, both NAA (p = 0.01) and Cr (p = 0.02) showed significant increases in their peak areas, while Cho was the only metabolite that showed significant increase in its peak height (p = 0.01).

Peak	%ΔH ± SE (*p*-value)		$\%\Delta\upsilon_{1/2}$ ± SE (*p*-value)		$\%\Delta A_S$ ± SE (*p*-value)	
	Single	Block	Single	Block	Single	Block
NAA	0.49 ± 0.18 (0.72)	1.09 ± 0.41 (0.14)	-5.59 ± 1.94 (0.07)	-1.09 ± 0.35 (0.45)	11.17 ± 1.94 (0.01)*	0.85 ± 0.47 (0.68)
Cr	0.78 ± 0.24 (0.53)	0.18 ± 0.09 (0.90)	-0.85 ± 0.28 (0.79)	-3.05 ± 0.97 (0.04)*	7.35 ± 0.94 (0.02)*	0.86 ± 0.35 (0.71)
Cho	2.24 ± 0.47 (0.01)*	1.41 ± 0.65 (0.25)	-2.10 ± 0.95 (0.73)	-2.62 ± 0.93 (0.12)	7.59 ± 0.84 (0.11)	2.09 ± 0.63 (0.54)

Table 4: *Average BOLD effects on the metabolites of higher relative abundance during visual stimulation*

**Significant BOLD effect observed*

The mean BOLD effects on the metabolites of lower relative abundance (i.e., Glu, Gln, and mI) from the four volunteers are shown in table 5. The significance of each average change is denoted by a p-value in parenthesis . The results indicate that none of these metabolites showed a significant BOLD effect in both paradigms (p > 0.05 in all comparisons).

Peak	% ΔH ± SE (*p*-value)		$\%\ \Delta\upsilon_{1/2}$ ± SE (*p*-value)		% ΔA_S ± SE (*p*-value)	
	Single	Block	Single	Block	Single	Block
Glu	0.24 ± 0.14 (0.90)	0.05 ± 0.02 (0.98)	-4.52 ± 0.78 (0.69)	-5.26 ± 1.28 (0.61)	0.57 ± 0.24 (0.95)	4.76 ± 0.57 (0.56)
Gln	1.61 ± 0.46 (0.29)	0.16 ± 0.07 (0.91)	-2.06 ± 0.79 (0.72)	-7.19 ± 1.24 (0.22)	14.59 ± 1.88 (0.05)	2.42 ± 0.68 (0.11)
mI	1.75 ± 0.38 (0.35)	1.23 ± 0.46 (0.35)	-1.82 ± 0.47 (0.69)	-1.03 ± 0.65 (0.74)	0.86 ± 0.39 (0.85)	2.92 ± 0.74 (0.32)

Table 5: *Average BOLD effects on the metabolites of lower relative abundance during visual stimulation.*

Discussion

Water Resonance fMRS

Theoretically, for both the cerebral water and metabolite resonances, averaging of spectral lines at NEX = 8 may be suitable in the case of conventional MRS acquisitions, but may impact on the amount of BOLD signal that could be recorded in fMRS. It is possible that during spectral averaging, some neural activity may not be captured, or that those lines acquired toward the end of the 'rest' and those acquired at the beginning of the 'stimulation' periods could be averaged together (especially in the "block" paradigm). This could then possibly lead to underestimation of the BOLD effects in the MR spectra. Indeed, consistent with theory, the BOLD effects on the water resonance were not found to be significant with the "block" paradigm; changes in height and linewidth (but not in area) with the "single" paradigm were however found to be significant. The insignificant change in the water spectral area, even though it responded to the BOLD effect, supports the use of the water signal as a reference standard in absolute quantification of the metabolite resonances using the standard NEX value of 8 in studies of healthy volunteers.

As was expected, the BOLD effects estimated in this study were lower than those estimated by Shih., *et al*. [7] and Zhu and Chen [6]. Whereas Zhu and Chen [6] conducted their study at 4 T and used only the "block" paradigm with an 8 Hz visual stimulus, Shih., *et al*. [7] performed their experiments at 3 T using both paradigms with a 6 Hz visual stimulus. Zhu and Chen [6] collected 20 averages in each of their five consecutive periods (designed as three OFF periods interleaved with two ON periods), resulting in a total of 100 spectra. For six

volunteers, they reported a mean (SE) percentage increase in the water peak height of 3.0 (0.4)% with corresponding linewidth percentage decrease of 2.3 (0.3)%. No change in the water peak area was reported. Shih., et al. [7] on the other hand, collected 128 averages in each of the rest and stimulus periods of their "single" paradigm; and 32 averages for each of their eight consecutive periods (designed as four ONs and four OFFs), resulting in 256 spectra. For five volunteers, they reported a mean (SE) percentage increase in peak height of 3.0 (0.5)%, associated with a linewidth decrease of 0.6 (0.1) Hz; the peak area increased by 0.8 (0.3)%. The estimated peak height and linewidth changes were said to be the same for both paradigms but it was unclear which paradigm gave the reported area change, which was comparable to the estimate from the "single" paradigm of this study (i.e. 1.12 (0.07)%).

Only %ΔH in the "single" paradigm of this study was higher than those of the above studies. The NEX value does not particularly affect the amount of neural activity; it only affects the way, and how much of, the resulting BOLD effect is recorded by the scanner. Therefore, the cause of this unexpectedly higher %ΔH observed in this study was unclear. Acquisitions in the rest and stimulation periods of the "single" paradigm were performed separately and not in a continuous way (as in the case of the six consecutive acquisitions of the "block" paradigm). After the rest scan, the scanner was re-shimmed and the visual activation scan was done. This could have offered two advantages: firstly, the volunteer had some rest between the "Off" and "On" acquisitions, and so could tolerate one acquisition after another with less movement and habituation effect [21]. Secondly, there is no possibility that the scanner will average any consecutive "Off" and "On" spectral lines together. This then gives two spectral line sets containing the pure "Off" and "On" effects. Therefore, a higher difference in peak heights between the two data sets could result. However, since this is the first study that has investigated the NEX = 8 effect, future studies may be required to further investigate the findings presented.

Volunteers in this study exhibited a wide variation in BOLD effects in the two paradigms; for instance, using the BOLD effects on the water resonance, the coefficient of variation, CoV for the two paradigms were ΔH = 42.92%, $\Delta\upsilon_{1/2}$ = 91.34%, and ΔA_S = 111.04% for the "single" paradigm, and ΔH = 68.58%, $\Delta\upsilon_{1/2}$ = 55.92%, and ΔA_S = 119.78% for the "block" paradigm. The generally significant inter-subject variability could be the result of differences in vascular architectures and cerebral blood volume changes induced by neural activity [24,25], plus differences in the tolerance levels (through motion and habituation effects) of the individual volunteers to the visual stimulation. This inherently large inter-volunteer variation in BOLD response may further impact on how the fMRS results among different studies compare.

Whereas Shih., *et al*. [7] used a variant of PRESS that collected the water and metabolite spectra simultaneously, this study used the standard PRESS sequence. The TE value also differed between this study (23 ms) and that of Shih., *et al*. (30 ms) [7], but was the same as that of Zhu and Chen [6]. The discrepancies between the results reported in this study and those of Shih., *et al*. [7] and Zhu and Chen [6] cannot be explained by the differences in the TE values or the order of the rest and stimulus periods in the paradigms [9]. There are however possible contributions of field strength [6], habituation effects due to prolonged stimulation (as with this study) [15,21], and the inherent inter-volunteer variability to these discrepancies. At a higher field strength, the susceptibility gradient that is associated with changes in T_2* increases, and so does the BOLD effect.

Metabolite Resonance fMRS

The BOLD effect alters the T_2* of both water and metabolite signals [6], and at higher fields ($B_o \geq 3$ T), this results in a small narrowing (0.2 - 0.3 Hz) of the spectral linewidth of all signals in the spectrum during neural stimulation. It is reported that this effect is mostly discernible on the strongest singlets of the methyl group of NAA and total Cr [18], particularly with the "single" activation paradigm. However, this study found a higher %ΔH for Cho than those for NAA and Cr in the "single" paradigm (Table 4).

In a functional MRS study at 7 T by Mangia., *et al*. [17], they simulated the BOLD effect on spectral line narrowing by applying line-broadening filters that increased spectral linewidth to 0.3 - 0.4 Hz (the same order of line narrowing due to the BOLD effect at 7 T). For most of the seventeen metabolite resonances they quantified *in vivo* (in two healthy subjects), they reported that the estimated concen-

trations systematically decreased by almost 1%. Thus their simulated BOLD changes (in those metabolites of interest in this study) were: NAA = 1.2%, Glu = 1.1%, Gln = 0.1%, Cr = 0.8%, Cho = 1.4% and mI = 1.0%. However, the non-simulated in vivo linewidth changes in this study were at least 1.2 Hz (about 3 times those simulated by Mangia., *et al*. [17]). It is therefore likely that the relatively high change in spectral linewidth reported in this study could be due to poor spectral resolution issues at 3 T since the actual T_2* change due to the BOLD effect is usually small at this field compared to 7 T [17]. Meanwhile, the percentage changes in the concentration of Cr (0.8%) reported by Mangia., *et al*. [17] compared with the "single" paradigm %ΔH result for Cr (0.78%) in this study (Table 4). The "block" paradigm %ΔH results in this study compared with the above concentration changes reported by Mangia., *et al*. [17] for NAA (1.09%), Cho (1.41%), Gln (0.16%), and mI (1.23%), where the values in the brackets are the changes estimated in this study; only the %ΔH change in Glu (0.24%) was found to be comparatively lower in this study (Tables 4-5). However, with the "block" paradigm, $\%\Delta A_s$ for Glu (4.76% ± 0.57) compared with its percentage concentration change elsewhere (3.0% ± 1.0) [18], also at 7 T.

For their "block" paradigm, Shih., *et al*. [7] reported average changes in the concentrations of Cho, NAA and Cr from five volunteers as 6.0%, 2.7% and 2.3% respectively. This study did not calculate metabolite concentrations but that should not cause any difference in the percentage BOLD changes between the two studies [9]. In the "block" paradigm of this study, percentage changes in A_S (which is proportional to concentration) for these three metabolites were relatively lower (Cho: 2.09%, NAA: 0.85%, Cr: 0.86%).

At 4 T, Zhu and Chen [6] used a paradigm of the form OFF-ON-OFF in their fMRS study to acquire eight and sixteen spectra in the rest and stimulation periods, respectively. They estimated the mean (SE) %ΔH and $\%\Delta\upsilon_{1/2}$ for NAA and Cr from six volunteers as: %ΔH; NAA = 2.5 (0.6), Cr = 3.1 (0.7); and $\%\Delta\upsilon_{1/2}$; NAA = 1.7 (0.5), Cr = 1.8 (0.5). The estimated %ΔH of the "block" paradigm in this study for both metabolites were comparatively lower but $\%\Delta\upsilon_{1/2}$ for NAA was similar between the two studies (1.7 ± 0.5 vs. 1.09 ± 0.35).

Mangia., *et al*. [18] reported a 3.0 (1)% increase in Glu concentration (from twelve healthy volunteers) at 7 T during the "single" paradigm. Their scanner was equipped with a quadrature transmit/receive half-volume RF coil with increased local sensitivity in the visual cortex. Their rest and stimulus periods lasted for 2.7 and 5.3 minutes, respectively. This study used equal rest and stimulus periods of 3.2 minutes in the "single" paradigm, and recorded a lower $\%\Delta A_S$ (which is proportional to concentration) of 0.57 (0.24)% in Glu. In their study, Mangia., *et al*. [18] observed that Glu exhibited a delayed response to the stimulus and manifested a general tendency of decreasing over time. If this is the case, then the lower percentage change in A_S observed in this study could be due to the shorter activation period of the "single" paradigm. The stimulation period was not long enough to cause significant BOLD response of Glu.

Conclusion

The results of this study suggest that MR spectral averaging using NEX = 8 yields estimated BOLD effects at 3 T that are comparable with those estimated at higher fields, where better temporal resolutions have been used and detection sensitivity is higher. This may be because NEX = 8 offers benefits of quicker signal averaging, which reduces motion-related artifacts in the data leading to better estimation accuracy of the BOLD effects on cerebral water and metabolite resonances. It thus appears that using a lower temporal resolution at lower fields may improve accuracy of the estimated BOLD effects. However, such a resolution often gives fewer data points to plot the time courses or patterns of the BOLD responses.

Acknowledgements

We wish to thank the Scottish Imaging Network, A Platform for Scientific Excellence (SINAPSE, 'Scottish Funding Council HR07020'), University of Glasgow (grant number: 11145801), and Sackler Institute of Psychological Research (grant number: 32660) for jointly funding the PhD research of Dr. A. N. Mumuni, which resulted, partly, in this report. Sincere thanks also go to Drs. Timo Schirmer and Ralph Noeske of GE Global Research Lab, Germany for their clarifications about the use of the SAGE software. We wish to also acknowledge the contribution of the study volunteers.

Conflict of Interest

The authors have no conflict of interest to declare.

Bibliography

1. Ogawa S., *et al*. "Brain magnetic resonance imaging with contrast dependent on blood oxygenation". *Proceedings of the National Academy of Sciences, USA* 87.24 (1990): 9868-9872.

2. Frahm J., *et al*. "Dynamic MR imaging of human brain oxygenation during rest and photic stimulation". *Journal of Magnetic Resonance Imaging* 2.5 (1992): 501-505.

3. Kwong KK., *et al*. "Dynamic magnetic resonance imaging of human brain activity during primary sensory stimulation". Proceedings of the National Academy of Science, USA 89.12 (1992): 5675-5679.

4. Blockley NP., *et al*. "A review of calibrated blood oxygenation level-dependent (BOLD) methods for the measurement of task-induced changes in brain oxygen metabolism". *NMR in Biomedicine* 26.8 (2013): 987-1003.

5. Malonek D and Grinvald A. "Interactions between electrical activity and cortical microcirculation revealed by imaging spectroscopy: implications for functional brain mapping". *Science* 272.5261 (1996): 551-554.

6. Zhu XH and Chen W. "Observed BOLD effects on cerebral metabolite resonances in human visual cortex during visual stimulation: a functional (1)H MRS study at 4 T". *Magnetic Resonance in Medicine* 46.5 (2001): 841-847.

7. Shih YY., *et al*. "INS-PRESS for functional MRS: simultaneous with-and without-water suppression spectral acquisition on visual cortex of human brains at 3T". *Proceedings of the International Society of Magnetic Resonance in Medicine* 17 (2009).

8. Hennig T., *et al*. "Detection of brain activation using oxygenation sensitive functional spectroscopy". *Magnetic Resonance in Medicine* 31.1 (1994): 85-90.

9. Mangia S and Tkac I. "Dynamic relationship between neurostimulation and N-acetylaspartate metabolism in the human visual cortex: evidence that NAA functions as a molecular water pump during visual stimulation". *Journal of Molecular Neuroscience: MN* 35.2 (2008): 245-248.

10. Song AW., *et al*. "Diffusion weighted fMRI at 1.5 T and 3 T". In: Proceedings of the 3rd Annual Meeting of the Society for Melanoma Research, Nice, France 457 (1995).

11. Menon RS., *et al*. "Functional MRI using the BOLD approach: field strength and sequence issues". In: Bihan, D.L. (ed). "Diffusion and perfusion magnetic resonance imaging". New York: Raven Press (1995): 327-334.

12. Wardlaw JM., *et al*. "A systematic review of the utility of 1.5 versus 3 tesla magnetic resonance brain imaging in clinical practice and research". *European Radiology* 22.11 (2012): 2295-2303.

13. Sarchielli P., *et al*. "Functional 1H-MRS findings in migraine patients with and without aura assessed interictally". *NeuroImage* 24.4 (2005): 1025-1031.

14. Drost DJ., *et al*. "Proton magnetic resonance spectroscopy in the brain: report of AAPM MR task group #9". *Medical Physics* 29.9 (2002): 2177-2197.

15. Fox PT and Raichle ME. "Stimulus rate determines regional brain blood-flow in striate cortex". *Annals of Neurology* 17.3 (1985): 303-305.

16. Baslow MH., *et al*. "Dynamic relationship between neurostimulation and N-acetylaspartate metabolism in the human visual cortex: evidence that NAA functions as a molecular water pump during visual stimulation". *Journal of Molecular Neuroscience: MN* 32.3 (2007): 235-245.

17. Mangia S., *et al*. "Sensitivity of single-voxel 1H-MRS in investigating the metabolism of the activated human visual cortex at 7 T". *Magnetic Resonance Imaging* 24.4 (2006): 343-348.

18. Mangia S., *et al*. "Sustained neuronal activation raises oxidative metabolism to a new steady-state level: evidence from 1H NMR spectroscopy in the human visual cortex". *Journal of Cerebral Blood Flow and Metabolism: Official Journal of the International Society of Cerebral Blood Flow and Metabolism* 27.5 (2007): 1055-1063.

19. Mumuni AN and McLean J. "Dynamic MR Spectroscopy of brain metabolism using a non-conventional spectral averaging scheme". *Journal of Neuroscience Methods* 277 (2017): 113-121.

20. Condon B., *et al*. "Habituation-like effects cause a significant decrease in response in MRI neuroactivation during visual stimulation". *Vision Research* 37.9 (1997): 1243-1247.

21. DeYoe EA., *et al*. "Functional magnetic resonance imaging (FMRI) of the human brain". *Journal of Neuroscience Methods* 54.2 (1994): 171-187.

22. Wright SM and Wald LL. "Theory and application of array coils in MR spectroscopy". *NMR in Biomedicine* 10.8 (1997): 394-410.

23. Press WH., *et al*. "Numerical recipes in C: the art of scientific computing". 2nd edition. Cambridge: Cambridge University Press (1992).

24. Ugurbil K., *et al*. "Functional mapping in the human brain using high magnetic fields". *Philosophical Transactions of the Royal Society of London. Series B: Biological Sciences* 354.1387 (1999): 1195-1213.

25. Weisskoff RM., *et al*. "Microscopic susceptibility variation and transverse relaxation: theory and experiment". *Magnetic Resonance in Medicine* 31.6 (1994): 601-610.

Volume 1 Issue 1 August 2017